



# Synthesis and Evaluation of [ $^{14}\text{C}$ ]-Labelled and Fluorescent-Tagged Paclitaxel Derivatives as New Biological Probes

Ch. Srinivasa Rao,<sup>ab</sup> Jao-Jia Chu,<sup>a</sup> Rai-Shung Liu<sup>b</sup> and Yiu-Kay Lai\*<sup>a</sup>

<sup>a</sup>Department of Life Science, National Tsing Hua University, Hsinchu, Taiwan 30043, Republic of China

<sup>b</sup>Department of Chemistry, National Tsing Hua University, Hsinchu, Taiwan 30043, Republic of China

Received 12 May 1998; accepted 7 August 1998

**Abstract**—Our present report deals with the preparation of *hitherto* unreported 7-((carbonyl- $^{14}\text{C}$ -acetyl)paclitaxel **4** and two new bioactive 7-substituted fluorescent taxoids (FITC **9** and rhodamine **11**), as well as evaluation towards their applications as biological probes. The results in this report demonstrate that (a) the new paclitaxel derivatives **4**, **9**, **11** could be prepared with good yields starting from paclitaxel; (b) the [ $^{14}\text{C}$ ]acetylation step was found to be better by using [ $^{14}\text{C}$ ]acetic anhydride rather than [ $^{14}\text{C}$ ]sodium acetate; (c) the radiochemical purity of **4** was 96% and its specific activity was 48 mCi/mmol; (d) the cytotoxicity of **4** was close to that of paclitaxel whereas **9**, **11** were far less active than paclitaxel, but these cytotoxic levels were good enough for their biological applications; (e) the drug-quantitation by flow cytometric analysis using **9** and **11** was proved to be equally efficient with respect to the radioactivity-based determination employing **4**; (f) the intracellular fluorescence mapping by **9** and **11** was found to be effective and the microtubule network pattern was visible in both the cases; (g) the overall fluorescence imaging efficiency was better with **11** while the intensity of fluorescence was higher with **9**; (h) staining of nucleolus was observed in fluorescence studies of both **9** and **11**. Based on these results, the newly prepared paclitaxel derivatives can be considered as efficient biological probes and should find further use in relevant applications. © 1998 Published by Elsevier Science Ltd. All rights reserved.

## Introduction

Paclitaxel (Taxol<sup>®</sup>), a highly functionalized diterpenoid plant product, is currently one of the most exciting leads in cancer chemotherapy.<sup>1</sup> Although the microtubule-targeted mitotic arrest of paclitaxel is well documented,<sup>2</sup> there is a lack of clear understanding about a number of secondary cellular effects caused by this drug. For instance, in macrophages, paclitaxel activates microtubule-associated protein kinase, increases tumor necrosis factor secretion, and decreases tumor necrosis factor receptor levels.<sup>3–7</sup> Moreover, recent results from our laboratory indicate that the apoptotic programs in paclitaxel treated HL-60 human leukemia cells can be initiated in either the G2/M or S phase through two different cytotoxic mechanisms,<sup>8</sup> and that paclitaxel induces hyperphosphorylation of vimentin intermediate

filaments in 9L rat brain tumor cells.<sup>9</sup> These findings suggest that there may be unexplored cellular targets for paclitaxel, and many intrinsic factors such as concentration, treatment time and intracellular accumulation of drug may contribute to the above mentioned activities of paclitaxel. In the light of these observations, we became interested in an investigation of the intracellular kinetics of paclitaxel and the resulting cytoskeletal alterations by using radio-labelled and fluorescent paclitaxel derivatives. While the [ $^3\text{H}$ ]-labelled paclitaxel derivatives were prepared and used for binding site localization and drug accumulation studies,<sup>10–15</sup> [ $^{14}\text{C}$ ]-labelled derivatives were thought to be more useful, particularly in pharmacokinetic studies, because of their high sensitivity and long half-life of the isotope. The fluorescent-conjugated paclitaxel derivatives previously used were mainly for microscopic studies, there has been no study to date concerning their utility for drug quantitation by flow cytometry. In the context of these aspects and also to meet our research needs, we felt that it is worthwhile to introduce new labels on the paclitaxel structure and evaluate their biological roles.

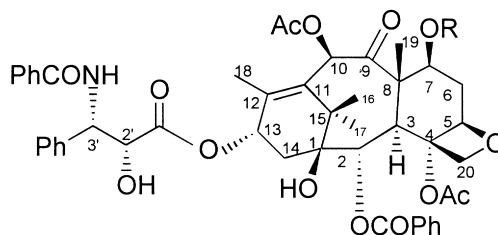
Key words: Antitumor compds; chemotherapy; fluorescence; labelling; substituent effects.

\*Corresponding author. Tel.: 886-3-5731095; Fax: 886-3-5715934; e-mail: lslyk@life.nthu.edu.tw

However, there are only a few synthetic methods available for [ $^{14}\text{C}$ ]paclitaxel derivatives: the *in vitro* production of minute amounts of [ $^{14}\text{C}$ ]paclitaxel;<sup>16,17</sup> preparation of [ $\text{N}3\text{'-}^{14}\text{C}$ ] and [ $\text{C}3\text{'-}^{14}\text{C}$ ]-labelled paclitaxel derivatives where the radio-labels were located on the C-13 side chain of paclitaxel<sup>18,19</sup> and a hemisynthesis of [ $3\text{'-}^{14}\text{C}$ ]taxotere.<sup>20</sup> It is worth noting that the preparation of these paclitaxel analogues with [ $^{14}\text{C}$ ]label on the side chain involved many steps. Moreover, there has been no report dealing with the synthesis of [ $^{14}\text{C}$ ]paclitaxel bearing the label on the diterpene ring. Since it has been shown that paclitaxel and 7-acetylpaclitaxel are similar in their ability to alter cell proliferation and microtubule polymerization,<sup>21–23</sup> and also that 7-epipaclitaxel is as active as paclitaxel,<sup>24</sup> we selected 7-([carbonyl- $^{14}\text{C}$ ]acetyl)paclitaxel as our candidate with a view to examine its capability in the determination of drug accumulation. Interestingly, this would be the first [ $^{14}\text{C}$ ]paclitaxel derivative bearing the radiolabel on the diterpene ring.

A variety of fluorescent ligands have been attached to paclitaxel previously, both on the side chain as well as on the ring skeleton and found to have a variable degree of success in terms of their cellular imaging efficiency.<sup>25–32</sup> Among these fluorophores, the fluorescein,<sup>27</sup> nitrobenzoyldiazo<sup>28</sup> (NBD) and Lissamine rhodamine B<sup>29</sup> dyes have produced good fluorescence images. We became interested in the examination of fluorescein isothiocyanate (FITC) because (a) it is a very commonly used dye in biology; (b) its excitation wavelength (488 nm) does not interfere with that of cellular proteins; (c) it is easily accessible and (d) it does not require either sophisticated microscopic instruments or special filters for fluorescence recording. In addition to FITC, the Lissamine rhodamine B was considered in order to make comparative study between their fluorescence abilities. To conjugate these two fluorophores on to the paclitaxel skeleton, esterification of C-7 hydroxyl position was found to be ideal on the basis of well-known structure-activity relationship studies.<sup>32–34</sup> Based on the previous finding that the C-7 substituted  $\alpha$ -amino acid ester derivatives of paclitaxel are unstable,<sup>35–37</sup> 6-aminocaproyl chain was chosen to serve as the linker between the paclitaxel and the fluorescent moiety. We reasoned that use of this long spacer arm would keep the bulky fluorophore away from the vicinity of the binding region of the paclitaxel skeleton and facilitate the drug to exhibit its usual cellular activity. This 6-carbon spacer arm was used earlier to conjugate the NBD dye to docetaxel and provided encouraging results.<sup>28</sup>

We herein report the synthesis of 7-([carbonyl- $^{14}\text{C}$ ]acetyl)paclitaxel **4** and two new 7-substituted fluorescent taxoids **9** and **11** (Fig. 1) and their evaluation as biological probes to study the intracellular drug quantitation



- 1**, R = H (paclitaxel)  
**4**, R =  $^{14}\text{C}\text{OCH}_3$   
**9**, R =  $\text{CO}(\text{CH}_2)_5\text{NH-FITC}$   
**11**, R =  $\text{CO}(\text{CH}_2)_5\text{NH-sulforhodamine}$

**Figure 1.** Structures of paclitaxel (**1**), [7- $^{14}\text{C}$ ]acetylpaclitaxel (**4**), FITC-paclitaxel (**9**), and rhodamine-paclitaxel (**11**).

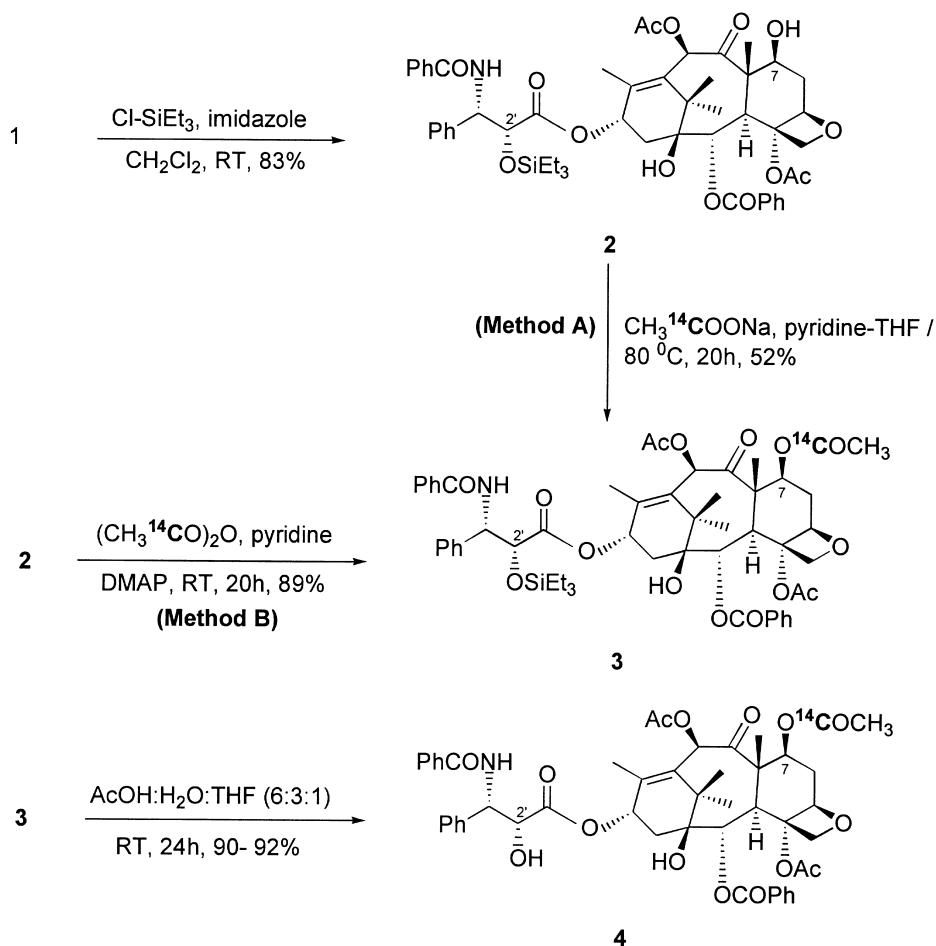
using **4**, **9** and **11**, as well as the visualization of cytoskeletal organization in tumor cultured cells with **9** and **11**.

## Results and Discussion

### Chemistry

The C-2'-OH of paclitaxel **1** is normally the most reactive and when it is protected, reaction usually proceeds selectively at the C-7 hydroxyl group. Thus, it was decided to replace the C-7 OH group of **2** with ester functions containing either carbon isotope or fluorophores conjugated through an aminocaproyl linker (Fig. 1).

**Synthesis of 7-([carbonyl- $^{14}\text{C}$ ]acetyl)paclitaxel.** Reaction of paclitaxel **1** with triethylsilyl chloride in  $\text{CH}_2\text{Cl}_2$  gave **2** in 83% yield (Scheme 1). The acetylation of C-7 OH group was performed by following a similar procedure (Method A),<sup>11</sup> wherein the acetic anhydride was generated *in situ* from radiolabelled sodium acetate in the presence of a catalytic amount of acetyl chloride. Thus, treatment of 2'-protected paclitaxel **2** with [ $^{14}\text{C}$ ]acetic anhydride, obtained as mentioned above, in dry pyridine and THF produced **3** in 52% yield and the radiochemical conversion was 38% (Scheme 1). The final step of deprotection at 2'-position of **3** was performed easily using a mixture of  $\text{AcOH-H}_2\text{O-THF}$  to obtain the desired **4** in 90% chemical yield. The structure of **4** was confirmed by comparing its spectral data with that of unlabelled 7-acetylpaclitaxel, and its radioactivity was 14.1 mCi/mmol i.e. 24% of the specific activity of [ $^{14}\text{C}$ ]sodium acetate used. Despite the successful preparation of **4**, a better method was sought for the acetylation step as the former procedure requires elevated temperature (80 °C), and an excess of isotopic reagent (5equiv of sodium acetate for 1equiv of **2**). In an alternate procedure (Method B, Scheme 1),



Scheme 1.

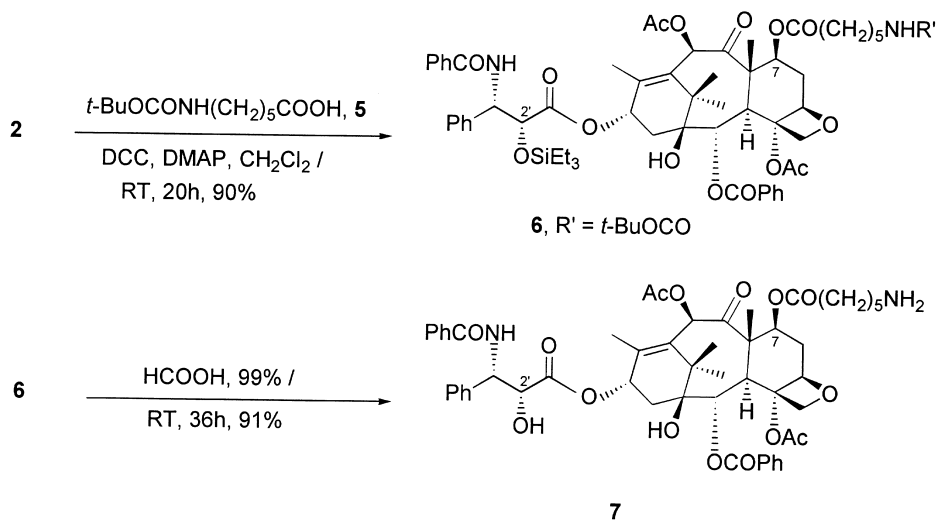
commercially available [<sup>14</sup>C]acetic anhydride was used instead of [<sup>14</sup>C]sodium acetate and it was found that the reaction could be carried out at room temperature with only 3 equivalents of isotopic reagent to obtain **3** in better chemical as well as radiochemical yields (89% and 45% respectively). Treatment of **3** with a mixture of AcOH-H<sub>2</sub>O-THF produced the target compound **4** at 92% chemical yield and its spectral characteristics were identical to the sample obtained from Method A. The radiochemical purity of **4** was 96% and its specific activity was 48 mCi/mmol (41% of the isotopic acetic anhydride). The compound **4** was stored as a methanolic solution at -20 °C and the product was found to be stable with very little radioactive decomposition.

**Synthesis of fluorescent-tagged taxoids.** The 2'-protected paclitaxel **2** was esterified at position C-7 with 6-(*N*-tert-butoxycarbonyl)aminocaproic acid **5**<sup>37</sup> in the presence of DCC and DMAP to give **6** in 90% yield (Scheme 2). Treatment of **6** with an excess of 99% formic acid at

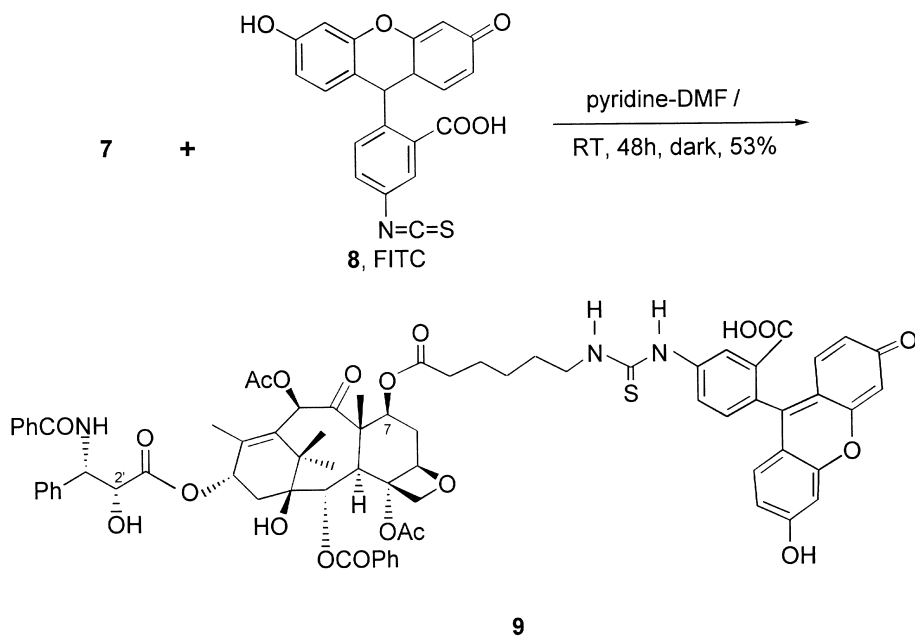
room temperature yielded 7-aminocaproylpaclitaxel **7** (91%), wherein both silyl and *N*-Boc protections were simultaneously removed (Scheme 2). The intermediate **7** was used to conjugate fluorescent labels on its amino functional group. Thus, the FITC dye **8** was conjugated to paclitaxel by reacting with **7** in DMF and pyridine at room temperature over 2 days in dark to afford the desired product **9** at 53% yield (Scheme 3). Similarly, the sulforhodamine analogue **11** was prepared at 58% yield from **7** by reacting with sulforhodamine B chloride **10** in 10% aqueous sodium bicarbonate and dioxane (Scheme 4). The structures of **9** and **11** were confirmed by their spectroscopic data and were found to be stable for at least two weeks when stored at -20 °C.

#### Biological evaluation studies

**Cytotoxicity assays.** In order to evaluate the cytotoxicity potentials of the prepared paclitaxel derivatives **4**, **7**, **9** and **11** relative to paclitaxel, cytotoxic assays were



Scheme 2.

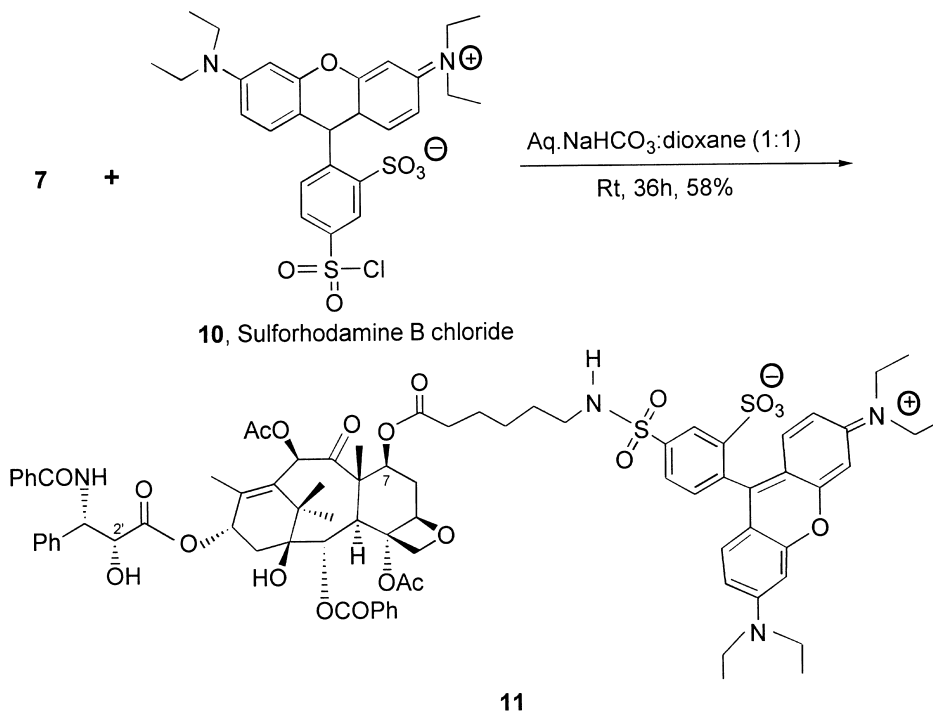


Scheme 3.

performed by testing their ability in the inhibition of the growth of H460 human non-small cell lung cancer (NSCLC) cells. We have employed the standard MTT assay<sup>38</sup> and determined the  $ID_{50}$  values (dose that reduced the final absorbance to 50% of control) from the survival curves (Fig. 2). The  $ID_{50}$  of **4** was close to that of paclitaxel thus confirm that derivatization at the C-7 position of paclitaxel by acetyl group retains significant activity. The FITC derivative **9** was found to be more cytotoxic than **7** and **11**, but less than **4**. The

cytotoxicity levels of **7** and **11** were almost equal and apparently the increased hydrophilic character of these derivatives might reduce their cell-permeability. From the above cytotoxicity data it was evident that these derivatives were less active than paclitaxel, but retain sufficient cytotoxicity to be suitable for carrying out biological applications.

**Drug accumulation studies.** The drug accumulation studies were undertaken in order to evaluate the abilities of



Scheme 4.

**4** (specific activity, 48 mCi/mmol), **9** and **11** in quantitating the intracellular drug accumulation. The assays were performed by treatment of these derivatives with the H460 culture cells with variable concentrations or treatment times.

The quantitation was conducted by using the radioactive counting for **4** or flow cytometric analysis for **9** and **11**. In the time-dependent experiments, the values of drug amounts retained by the H460 tumor cells were plotted against the time-scale and the drug saturation points were then determined (Figs 3A and 4A). The accumulation of **4** was increased steadily during a 1 h period and the saturation point was reached after 6 h of treatment (Fig. 3A). Similarly, the saturation level for **9** and **11** was attained after 6 h (Fig. 4A). In the case of the dose-dependent experiments, **4** needed 0.1 mM for its saturation level (Fig. 3B) while saturation concentration was 0.1 and 0.01 mM for **9** and **11** respectively (Fig. 4B). The finite variations in the concentrations required for saturation points of **9** and **11** may be either due to the differences in their sensitivities or because of their variable drug-uptake levels. However, the results clearly demonstrate that the fluorescence-based quantitation is almost similar when compared to radioactive determination and could be useful as a complementary tool for the drug quantitation studies.

**Fluorescence studies.** To establish the fluorescent mapping efficiency of **9** and **11**, drug-treatment protocols were performed using H460 NSCLC culture cells. Different doses and treatment periods were followed in the reported protocols to get the ideal results. While one group used 10  $\mu\text{M}$  during 6 h exposure, another group required 20  $\mu\text{M}$  for 2 h to draw better results.<sup>29</sup> Both of these reported scales were not suitable for our experiments. As the tumor cultures under study were not the same, these differences could be regarded as the protocol variations. The cells were treated with **9** or **11** and then fluorescence was observed after fixing the interphasic cells in ethanol. It was observed that the concentration and the treatment time have profound effects on the fluorescence pattern of cellular organization as well as the illumination levels. Also, **9** and **11** required different doses and treatment periods in order to obtain optimal results. The FITC-paclitaxel showed good fluorescence pattern when the tumor cells were incubated with 0.1  $\mu\text{M}$  of **9** for 2 h at 4°C, whereas a much higher dose (10  $\mu\text{M}$ ) of **11** was needed for obtaining good images with rhodamine-paclitaxel. This difference in the corresponding doses of **9** and **11** may be due to variations in their cytotoxicity and drug uptake level. Under these optimal conditions, the cells displayed fluorescent microtubule networks (Fig. 5) and both **9** and **11** have exhibited the microtubule organizing centers (MTOCs). However, the microtubule filamentous

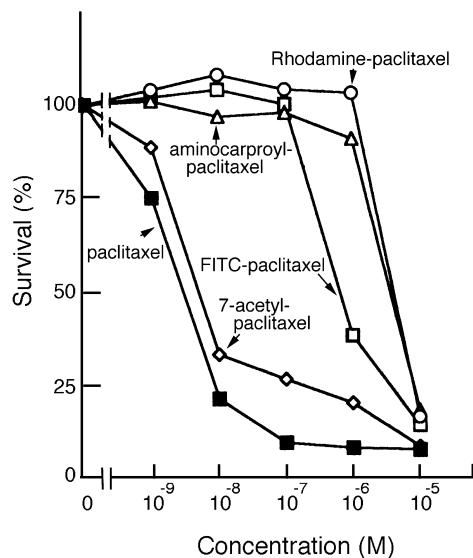


**Figure 2.** Inhibition of the growth of H-460 cells by **4**, **7**, **9** and **11** relative to paclitaxel: Cells were grown in culture in the presence of various concentrations of paclitaxel derivatives for 4 days and an MTT assay was performed. One hundred percent represents the number of cells present in the control culture.

structures appeared to be slightly different from the corresponding immunofluorescence stain.

It is interesting to note that two aspects of our results are similar to that of Lissamine rhodamine taxoid as used by Nicolaou's group.<sup>29</sup> The first and most striking similarity is regarding the staining of nucleoli by **9** and **11** and the second indication is related to the presence of few diffused background signals. This identical mode of fluorescence pattern could be expected for our rhodamine paclitaxel **11** as it is the same fluorophore as that used by the above group except that it is linked to the paclitaxel skeleton by a much longer carbon chain in our studies. Surprisingly, the FITC-labelled paclitaxel **9** also exhibited similar phenomena and thus supports the view that there may be undetected targets for paclitaxel other than tubulin. However, a different reason was put forward by Guenard et al. for the staining of nuclei when they used the NBD-labelled docetaxel, and they attributed the findings thereof due to cytological techniques.<sup>28</sup> While these effects were observed only under cell fixation procedures with NBD-docetaxel, the reported results with rhodamine-conjugated paclitaxel demonstrated under both living and fixation protocols. Interestingly, the fluorescein-labelled paclitaxel used by another group did not display the fluorescence of the nucleolus.<sup>27</sup> Further investigations are necessary to clarify these discrepancies and to provide a better understanding about these observations. The findings from previous reports and our present study reveal that

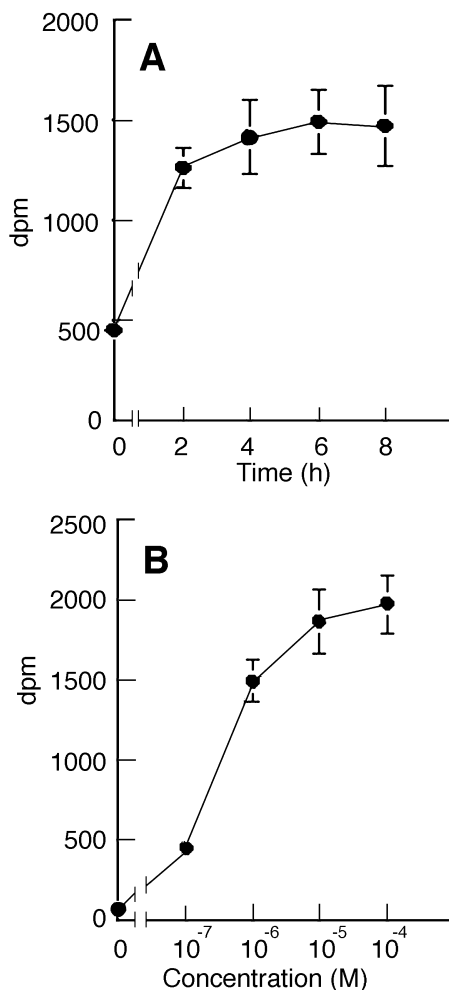


**Figure 3.** Drug accumulation using radioactive paclitaxel **4**. (A) Time-dependent accumulation: Treatment of H-460 cells with 1  $\mu$ M of **4** for different time periods. The cells were collected at the indicated time periods and the radioactivity was determined using  $\beta$ -scintillation counting. (B) Dose-dependent accumulation: Treatment of H-460 cells for 3 h with different indicated doses of **4**.

the staining patterns of fluorescent taxoids may not necessarily depend on the structure of the fluorophore. This is clearly evident from the observations that (a) the structure of FITC closely resembles the fluorescein dye but the performance of FITC-taxoid **9** was similar to the rhodamine analogue **11** (b) while the change in the spacer arm linking the fluorophore to the paclitaxel provided different results when fluorescein dye was employed,<sup>27,29</sup> not much effect was observed in the case of the rhodamine fluorophore.

Our results from **9** and **11** indicate that the fluorescence pattern appeared to be similar in both cases but **11**

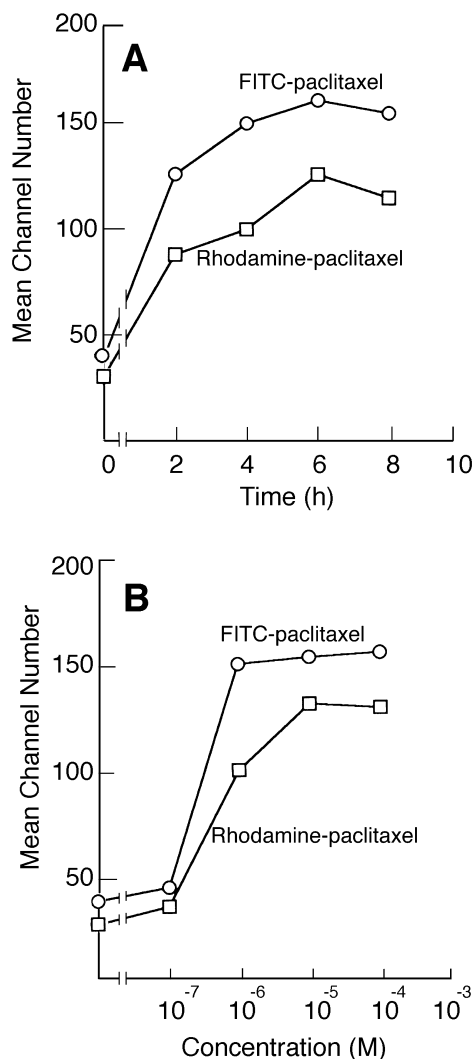


**Figure 4.** Drug accumulation using fluorescent taxoids **9** and **11**. (A) Time-dependent accumulation: Treatment of H-460 cells with 1  $\mu$ M of **9** and **11** for indicated time periods. The cells were collected at these intervals and flow cytometry analysis was performed for quantitation. (B) Dose-dependent accumulation: Treatment of H-460 cells for 3 h with indicated doses of **9** and **11**.

offers a better overall fluorescence image for the microtubule network than **9**. However, the fluorescence level of **9** was found to be much higher than that of **11**. Both **9** and **11** have delivered good fluorescence abilities and thus suitable for further sub-cellular localization studies.

### Conclusion

Although the microtubule-targeted activity of paclitaxel has been extensively studied, a number of non-mitotic

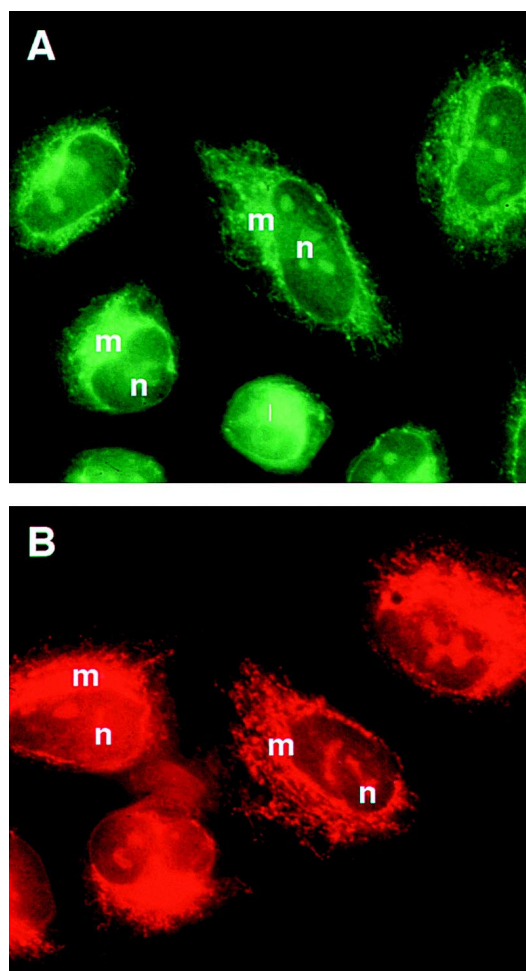


**Figure 5.** Fluorescence microscopy image of permeabilized and fixed H-460 cells at interphase. (A) FITC-paclitaxel **9** staining; (B) rhodamine paclitaxel **11** staining; m, microtubule organizing center (MTOC); n, nucleolus.

actions of paclitaxel have been observed recently. Understanding of these new actions of paclitaxel is very important for its better practical therapy and therefore, warrants further research in this direction. The intracellular localization studies are thus essential to elucidate the molecular mechanism(s) involved in these processes. The bio-tracer investigations using radioactive and fluorescent-labelled paclitaxel derivatives attain significance in this respect as valuable tools to determine the cellular events. In pursuit of this goal, our present efforts are directed to seek for novel potential labelling groups to conjugate to paclitaxel. The synthetic results show that the desired paclitaxel derivatives **4**, **9** and **11** could be prepared in good yields starting from paclitaxel. The 7-([carbonyl-<sup>14</sup>C]-acetyl)paclitaxel **4** was obtained in very good chemical yield as well as radiochemical activity when the acetylation was carried out

using [ $^{14}\text{C}$ ]acetic anhydride in place of [ $^{14}\text{C}$ ]sodium acetate. The specific activity of **4** (obtained from Method B) was determined to be 48 mCi/mmol and it was found to be sufficient enough for drug accumulation studies. This is the first report for the preparation of [ $^{14}\text{C}$ ]paclitaxel having its radiolabel on the taxane ring skeleton. The fluorescent paclitaxel derivatives **9** and **11** were prepared from a common intermediate **7** and they were chemically stable when stored at  $-20^\circ\text{C}$ . The cytotoxicity levels for these derivatives were lower than that of paclitaxel, but sufficient for their use as biological probes. We have demonstrated for the first time that the fluorescent taxoids could be used for drug quantitation. The drug accumulation experiments reveal that a close homology exists between the results of radioactive and flow cytometric analyses and prove that these probes could be of more utility for further related studies. The fluorescence microscopy results from **9** and **11** were successful in displaying the microtubule network, and a noteworthy feature is the staining of nucleolus. The results also indicate that the fluorescence-mapping pattern of labelled taxoids is not completely identical to the corresponding anti-tubulin antibody stain and thus helpful in determining unexplored targets of paclitaxel.

### Experimental

**Chemical materials and methods.** All reactions were carried out in a nitrogen atmosphere under anhydrous conditions, unless otherwise mentioned. Commercially available reagents were used without further purification. [ $^{14}\text{C}$ ]Acetic acid, sodium salt and [ $^{14}\text{C}$ ]acetic anhydride were purchased from Amersham International plc (England). The [ $^{14}\text{C}$ ]acetic acid, sodium salt was supplied as an aqueous solution (specific activity, 59.0 mCi/mmol; radioactive concentration, 200  $\mu\text{Ci}/\text{ml}$ ; radiochemical purity, 98.6%) and was stored at  $2^\circ\text{C}$ . The [ $^{14}\text{C}$ ]acetic anhydride was supplied in borosilicate glass break-seal ampules sealed under vacuum [specific activity, 118 mCi/mmol; radiochemical purity, 98.6%] and stored at  $-20^\circ\text{C}$ . Fluorescein isothiocyanate (FITC), isomer 1 (5 isomer) and sulforhodamine B were purchased from Aldrich Chemical Company Inc (USA) and they were stored under prescribed conditions. All the prepared paclitaxel derivatives were stored at  $-20^\circ\text{C}$ . Solvents were dried and purified before use. Thin-layer chromatography was carried out using aluminum-backed silica gel plates (Merck-60F $_{254}$ ). Developed TLC plates were viewed under UV detector (Spectroline; model, ENF 240). Radiochemical purity was done by analytical thin-layer chromatography and the radioactive TLC plates were scanned on a Berthold Model LB 511. Radioactive measurements were performed using a PACKARD 1600 TR liquid scintillation analyzer and

the specific activity was determined with an IN/US  $\beta$ -RAM System (2  $\mu\text{L}$  aliquots in 1 mL of Aquasol II, New England Nuclear). NMR spectra were recorded on Bruker AMX-300 and AMX-400 instruments and calibrated using TMS as internal standard. Multiplicities were recorded by the following abbreviations: s, singlet; d, doublet; dd, double doublet; t, triplet; q, quartet, m, multiplet; br, broad; band, overlapping signals. Chemical shifts were expressed in parts per million (ppm). Coupling constants ( $J$ ) were given in Hertz (Hz).

**2'-Triethylsilylpaclitaxel 2.** To a well-stirred solution of paclitaxel **1** (527 mg, 0.62 mmol) and imidazole (460 mg, 6.75 mmol) in  $\text{CH}_2\text{Cl}_2$  (12 mL) at room temperature was added  $\text{Et}_3\text{SiCl}$  (0.15 mL, 0.99 mmol) slowly under a nitrogen atmosphere. After stirring the reaction mixture for 30 min, the reaction was quenched with water (15 mL), and the organic layer was separated, dried and concentrated under reduced pressure. The crude product was then passed through a short silica gel column (hexane/EtOAc, 2:3;  $R_f=0.58$ ) to give 2'-triethylsilyloxy-paclitaxel **2** (496 mg, 83%) as a colorless powder:  $^1\text{H}$  NMR (400 MHz,  $\text{CDCl}_3$ )  $\delta$  0.37–0.49 (m, 6H,  $\text{SiCH}_2\text{CH}_3$ ), 0.80 (t,  $J=7.9$ , 9H,  $\text{SiCH}_2\text{CH}_3$ ), 1.12 (s, 3H,  $\text{H}_{16}$ ), 1.23 (s, 3H,  $\text{H}_{17}$ ), 1.67 (s, 3H,  $\text{H}_{18}$ ), 1.71–1.74 (m, 1H,  $\text{H}_{6b}$ ), 1.92 (s, 3H,  $\text{H}_{19}$ ), 2.11–2.19 (m, 2H,  $\text{H}_{14}$ ), 2.23 (s, 3H,  $\text{C}_{10}\text{-CH}_3\text{CO}$ ), 2.32–2.55 (m,  $\text{H}_{6a}$ ), 2.54 (s, 3H,  $\text{C}_4\text{-CH}_3\text{CO}$ ), 3.80 (d,  $J=7.0$ , 1H,  $\text{H}_3$ ), 4.21 (d,  $J=8.5$ , 1H,  $\text{H}_{20}$ ), 4.30 (d,  $J=8.5$ , 1H,  $\text{H}_{20}$ ), 4.41 (dd,  $J=10.6$ , 6.6, 1H,  $\text{H}_7$ ), 4.67 (d,  $J=1.9$ , 1H,  $\text{H}_2$ ), 4.96 (d,  $J=8.0$ , 1H,  $\text{H}_5$ ), 5.67–5.70 (m, 2H,  $\text{H}_3'$  and  $\text{H}_2$ ), 6.25 (t,  $J=8.8$ , 1H,  $\text{H}_{13}$ ), 6.28 (s, 1H,  $\text{H}_{10}$ ), 7.09 (d,  $J=8.6$ , 1H, NH), 7.31–7.58 (m, 11H, ArH), 7.64 (d,  $J=8.0$ , 2H, ArH), 8.13 (d,  $J=8.0$ , 2H, ArH);  $^{13}\text{C}$  NMR (100 MHz,  $\text{CDCl}_3$ )  $\delta$  4.4, 6.5, 14.8, 20.8, 22.3, 23.0, 26.8, 35.6, 35.9, 43.3, 45.6, 55.7, 58.6, 71.5, 72.1, 74.9, 75.2, 75.6, 76.5, 79.2, 81.2, 84.5, 126.5, 127.0, 128.0, 128.6, 128.7, 128.8, 129.3, 130.2, 131.7, 133.0, 133.6, 134.2, 138.5, 142.5, 166.9, 167.0, 170.1, 171.2, 171.5, 203.7. Anal. calcd for  $\text{C}_{53}\text{H}_{65}\text{NSiO}_4$ : C, 65.75; H, 6.77; N, 1.44. Found: C, 65.59; H, 6.61; N, 1.24.

**2'-Triethylsilyl-7-([carbonyl- $^{14}\text{C}$ ]acetyl)paclitaxel 3.** (Method A): The commercial [ $^{14}\text{C}$ ]sodium acetate [supplied as an aqueous solution; 101  $\mu\text{mol}$ ; specific activity, 59 mCi/mmol] was introduced into a two-neck round-bottom flask and water was removed under vacuum. It was heated at  $190^\circ\text{C}$  for 1 h under reduced pressure (0.01 mm/Hg) and then the heating was stopped and the material was allowed to reach room temperature. Then, THF (1 mL) and acetyl chloride (8  $\mu\text{L}$ ) were added and the mixture was stirred overnight at room temperature. To the milky suspension that resulted, **2** (19 mg, 20  $\mu\text{mol}$ ) dissolved in dry pyridine (0.2 mL) was added and the mixture was heated at  $80^\circ\text{C}$  for 20 h. The solvents were removed by flushing with a stream of

nitrogen and the crude material was treated with water (3×2 mL) and extracted with CH<sub>2</sub>Cl<sub>2</sub> (3×5 mL). The combined organic extract was concentrated under vacuum and the preparative TLC on silica gel (EtOAc/hexanes, 1:2; R<sub>f</sub>=0.65) afforded the product **3** as a colorless solid (11 mg, 52%). (*Method B*): To a solution of **2** (31 mg, 30 μmol) in dry pyridine (0.5 mL) at room temperature under nitrogen atmosphere were added DMAP (0.1 mg, *catalytic*) and [<sup>14</sup>C]acetic anhydride (90 μmol; specific activity, 118 mCi/mmol). The reaction mixture was stirred at room temperature for 20 h and evaporated to dryness. The residue was treated with water (3×5 mL) and extracted with CH<sub>2</sub>Cl<sub>2</sub> (3×8 mL). The combined organic extract was concentrated under reduced pressure and the crude material was purified by preparative TLC on silica gel (EtOAc/hexanes, 1:2; R<sub>f</sub>=0.65) to give **3** (27 mg, 89%). The TLC R<sub>f</sub> of **3** from both the methods was found to be identical and the chromatographic behavior was similar to the authentic unlabelled sample. The radiochemical purity of **3** was determined to be 98% and the NMR spectra were found to be identical by comparing with an authentic unlabelled sample. <sup>1</sup>H NMR (400 MHz, CDCl<sub>3</sub>) δ 0.37–0.48 (m, 6H, 6H, SiCH<sub>2</sub>CH<sub>3</sub>), 0.80 (t, *J*=8.0, 9H, SiCH<sub>2</sub>CH<sub>3</sub>), 1.14 (s, 3H, H<sub>16</sub>), 1.19 (s, 3H, H<sub>17</sub>), 1.74 (s, 3H, H<sub>18</sub>), 1.77–1.83 (m, 1H, H<sub>6b</sub>), 1.95 (s, 3H, H<sub>19</sub>), 2.01 (s, 3H, C<sub>7</sub>-CH<sub>3</sub>CO), 2.12–2.19 (m, 1H, H<sub>14</sub>), 2.24 (s, 3H, C<sub>10</sub>-CH<sub>3</sub>CO), 2.38–2.48 (m, 1H, H<sub>14</sub>), 2.52 (s, 3H, C<sub>4</sub>-CH<sub>3</sub>CO), 2.53–2.64 (m, 1H, H<sub>6a</sub>), 3.90 (d, *J*=7.0, 1H, H<sub>3</sub>), 4.18 (d, *J*=8.5, 1H, H<sub>20</sub>), 4.32 (d, *J*=8.5, 1H, H<sub>20</sub>), 4.68 (d, *J*=1.6, 1H, H<sub>27</sub>), 4.94 (d, *J*=8.0, 1H, H<sub>5</sub>), 5.60 (dd, *J*=10.6, 6.6, 1H, H<sub>7</sub>), 5.67 (d, *J*=6.0, 2H, H<sub>3'</sub> and H<sub>2</sub>), 6.20 (t, *J*=8.5, 1H, H<sub>13</sub>), 6.26 (s, 1H, H<sub>10</sub>), 7.10 (d, *J*=8.0, 1H, NH), 7.30–7.61 (m, 11H, ArH), 8.11 (d, *J*=8.0, 2H, ArH); <sup>13</sup>C NMR (100 MHz, CDCl<sub>3</sub>) δ 4.3, 6.4, 10.8, 14.5, 20.7, 21.0, 22.9, 26.4, 33.3, 35.6, 41.2, 43.4, 46.9, 55.7, 56.0, 71.3, 74.5, 74.7, 75.3, 76.3, 76.5, 76.7, 76.8, 77.6, 81.0, 84.0, 126.5, 127.0, 128.1, 128.8, 129.1, 130.2, 131.7, 132.7, 133.7, 140.9, 166.9, 167.1, 168.9, 169.8, 170.4, 171.8, 202.6.

**7-([Carbonyl-<sup>14</sup>C]-acetyl)paclitaxel 4.** To 2'-Triethylsilyl-7-([carbonyl-<sup>14</sup>C]-acetyl)paclitaxel **3** [obtained from method A or method B; 10 mg, 9.9 μmol), was added to a mixture of acetic acid (0.6 mL), water (0.3 mL), and THF (0.1 mL) and the contents were stirred at room temperature for 24 h (monitored by TLC). The reaction solution was then treated with aqueous NaHCO<sub>3</sub> (3 mL) and extracted with EtOAc (3×4 mL). The combined organic extract was dried (Na<sub>2</sub>SO<sub>4</sub>), and the crude compound was purified by preparative TLC (EtOAc/hexanes, 1:2; R<sub>f</sub>=0.44) to afford 7-([carbonyl-<sup>14</sup>C]-acetyl)paclitaxel **4** as a white powder (7.0 mg, 90%). The TLC R<sub>f</sub> and NMR spectra of **4** were consistent with that of unlabelled 7-acetylpaclitaxel. <sup>1</sup>H NMR (400 MHz, CDCl<sub>3</sub>) δ 1.12 (s, 3H, H<sub>16</sub>), 1.16 (s, 3H, H<sub>17</sub>), 1.78 (s,

6H, H<sub>18</sub> and H<sub>19</sub>), 1.77–1.89 (m, 1H, H<sub>6b</sub>), 2.06 (s, 3H, C<sub>7</sub>-CH<sub>3</sub>CO), 2.14 (s, 3H, C<sub>10</sub>-CH<sub>3</sub>CO), 2.29–2.38 (m, 2H, H<sub>14</sub>), 2.40 (s, 3H, C<sub>4</sub>-CH<sub>3</sub>CO), 2.42–2.58 (m, 1H, H<sub>6a</sub>), 3.92 (d, *J*=7.0, 1H, H<sub>3</sub>), 4.18 (d, *J*=8.0, 1H, H<sub>20</sub>), 4.34 (d, *J*=8.0, 1H, H<sub>20</sub>), 4.79 (d, *J*=2.4, 1H, H<sub>27</sub>), 4.94 (d, *J*=7.0, 1H, H<sub>5</sub>), 5.55 (dd, *J*=10.0, 4.5, 1H, H<sub>7</sub>), 5.68 (d, *J*=7.0, 1H, H<sub>3'</sub>), 5.80 (d, *J*=7.0, 1H, H<sub>2</sub>), 6.18 (t, *J*=8.5, 1H, H<sub>13</sub>), 6.26 (s, 1H, H<sub>10</sub>), 7.16 (d, *J*=8.0, 1H, NH), 7.28–7.68 (m, 11H, ArH), 7.74 (d, *J*=8.0, 2H, ArH), 8.10 (d, *J*=7.3, 2H, ArH); <sup>13</sup>C NMR (100 MHz, CDCl<sub>3</sub>) δ 10.8, 14.6, 20.7, 20.8, 21.0, 22.5, 26.6, 33.4, 35.6, 43.2, 47.0, 54.9, 56.1, 71.4, 72.0, 73.2, 73.3, 74.3, 75.5, 76.4, 76.5, 76.6, 78.4, 81.1, 84.0, 84.1, 127.0, 128.2, 128.7, 128.9, 129.1, 130.1, 131.9, 133.0, 133.7, 134.0, 138.0, 140.3, 150.4, 166.9, 168.9, 170.3, 170.4, 172.4, 201.8.

**6-N-ter-Butoxycarbonylaminocaproic acid 5.** Prepared from 6-aminocaproic acid and di-*ter*-butyl dicarbonate in MeOH in the presence of NEt<sub>3</sub> using reported procedure.<sup>37</sup> <sup>1</sup>H NMR (300 MHz, CDCl<sub>3</sub>) δ 1.31–1.46 (m, 13H, *ter*-butyl-CH<sub>3</sub> and CH<sub>2</sub>), 1.55–1.64 (m, 2H, CH<sub>2</sub>), 2.29 (br t, 2H, CH<sub>2</sub>), 3.01–3.07 (m, 2H, NCH<sub>2</sub>), 4.63 (br s, 1H, NH).

**2'-Triethylsilyl-7-(tert-butoxycarbonylaminocaproyl)paclitaxel 6.** To a solution of **2** (48 mg, 0.05 mmol, 1 equiv) and DMAP (6 mg, 0.05 mmol, 1 equiv) in CH<sub>2</sub>Cl<sub>2</sub> (5 mL) at room temperature under nitrogen was sequentially treated with **5** (52 mg, 0.225 mmol, 4.5 equiv) and DCC (198 mg, 0.225 mmol, 4.5 equiv). The mixture was stirred at room temperature for 20 h and then diluted with CH<sub>2</sub>Cl<sub>2</sub> (10 mL) and filtered to remove the urea. The filtrate was concentrated under reduced pressure and the resulting residue was passed through a silica gel column (EtOAc/hexanes, 1:1) to afford **6** as a colorless solid (53 mg, 90%). <sup>1</sup>H NMR (300 MHz, CDCl<sub>3</sub>-CD<sub>3</sub>OD) δ 0.33–0.46 (m, 6H, SiCH<sub>2</sub>CH<sub>3</sub>), 0.82 (t, *J*=7.5, 9H, SiCH<sub>2</sub>CH<sub>3</sub>), 1.06–1.28 (m, 4H, CH<sub>2</sub>), 1.14 (s, 3H, H<sub>16</sub>), 1.21 (s, 3H, H<sub>17</sub>), 1.29–1.34 (m, 9H, *ter*-butyl CH<sub>3</sub>), 1.57–1.62 (m, 2H, CH<sub>2</sub>), 1.64–1.68 (m, 1H, H<sub>6b</sub>), 1.76 (s, 3H, H<sub>19</sub>), 1.95–1.99 (m, 2H, CH<sub>2</sub>), 2.02 (s, 3H, H<sub>18</sub>), 2.11 (s, 3H, C<sub>10</sub>-CH<sub>3</sub>CO), 2.12–2.23 (m, 2H, H<sub>14</sub>), 2.28–2.39 (m, 1H, H<sub>6a</sub>), 2.47 (s, 3H, C<sub>4</sub>-CH<sub>3</sub>CO), 3.02–3.08 (m, 2H, NCH<sub>2</sub>), 3.92 (d, *J*=6.0, 1H, H<sub>3</sub>), 4.14 (d, *J*=8.0, 1H, H<sub>20</sub>), 4.30 (d, *J*=8.0, 1H, H<sub>20</sub>), 4.59–4.68 (m, 1H, H<sub>27</sub>), 4.93 (d, *J*=8.0, 1H, H<sub>5</sub>), 5.54 (dd, *J*=6.5, 1.2, 1H, H<sub>7</sub>), 5.68 (d, *J*=7.0, 1H, H<sub>2</sub>), 5.91 (m, 1H, H<sub>3'</sub>), 6.21 (t, *J*=6.0, 1H, H<sub>13</sub>), 6.26 (s, 1H, H<sub>10</sub>), 7.16 (d, *J*=8.0, 1H, NH), 7.29–7.58 (m, 11H, ArH), 7.72 (d, *J*=8.0, 2H, ArH), 8.10 (d, *J*=8.0, 2H, ArH); <sup>13</sup>C NMR (100 MHz, CDCl<sub>3</sub>-CD<sub>3</sub>OD) δ 4.4, 6.6, 10.9, 14.2, 20.4, 20.8, 22.0, 24.2, 26.5, 26.8, 28.4, 30.0, 30.2, 33.5, 33.9, 35.8, 43.1, 43.2, 43.9, 46.7, 54.7, 56.1, 56.6, 71.8, 72.0, 73.5, 74.4, 75.2, 76.4, 76.6, 78.6, 80.2, 81.1, 83.8, 84.2, 126.9, 127.4,

128.8, 129.3, 130.2, 131.5, 133.0, 133.5, 134.0, 140.2, 150.6, 167.2, 168.5, 170.2, 172.2, 202.3. Anal. calcd for  $C_{64}H_{84}N_2SiO_{17}$ : C, 65.06; H, 7.16; N, 2.37. Found: C, 65.18; H, 7.01; N, 2.45.

**7-(Aminocaproyl)paclitaxel 7.** A mixture of **6** (50 mg, 0.04 mmol) and 99% formic acid (2 mL) was stirred at room temperature under nitrogen for 36 h. The excess of the reagent was removed under vacuum and 10% aqueous  $NaHCO_3$  ( $2 \times 10$  mL) was added to the residue. This was then extracted with EtOAc ( $2 \times 15$  dried ( $Na_2SO_4$ ) and concentrated. The preparative TLC of the crude material on silanized silica gel (EtOAc/petroleum ether, 2:1;  $R_f=0.39$ ) afforded **7** as a colorless solid (35 mg, 91%).  $^1H$  NMR ( $CDCl_3-CD_3OD$ )  $\delta$  1.13 (s, 3H,  $H_{16}$ ), 1.22 (s, 3H,  $H_{17}$ ), 1.19–1.29 (m, 4H,  $CH_2$ ), 1.52–1.56 (m, 2H,  $CH_2$ ), 1.58–1.61 (m, 1H,  $H_{6b}$ ), 1.70 (s, 3H,  $H_{19}$ ), 1.73 (s, 3H,  $H_{18}$ ), 1.74–1.87 (m, 2H,  $CH_2$ ), 2.16 (s, 3H,  $C_{10}-CH_3CO$ ), 2.19–2.31 (m, 2H,  $H_{14}$ ), 2.39 (s, 3H,  $C_4-CH_3CO$ ), 2.36–2.51 (m, 1H,  $H_{6a}$ ), 3.05–3.14 (m, 2H,  $NCH_2$ ), 3.90 (d,  $J=7.0$ , 1H,  $H_3$ ), 4.16 (d,  $J=8.0$ , 1H,  $H_{16}$ ), 4.25 (d,  $J=8.0$ , 1H,  $H_{16}$ ), 4.78–4.81 (m, 1H,  $H_2$ ), 4.95 (d,  $J=8.0$ , 1H,  $H_5$ ), 5.58 (dd,  $J=9.0$ , 1.5, 1H,  $H_7$ ), 5.64 (d,  $J=7.0$ , 1H,  $H_2$ ), 5.84 (dd,  $J=7.5$ , 1.0, 1H,  $H_3$ ), 6.20 (t,  $J=7.0$ , 1H,  $H_{13}$ ), 6.25 (s, 1H,  $H_{10}$ ), 7.29–7.58 (m, 12H, ArH and NH), 7.62 (d,  $J=8.0$ , 2H, ArH), 8.09 (d,  $J=8.0$ , 1H, ArH);  $^{13}C$  NMR (100 MHz,  $CDCl_3-CD_3OD$ )  $\delta$  11.0, 14.4, 20.6, 20.8, 22.2, 24.1, 26.4, 30.1, 33.3, 33.5, 33.8, 35.6, 43.1, 43.2, 43.8, 46.9, 54.9, 56.2, 56.6, 71.6, 72.1, 73.3, 74.5, 75.4, 76.6, 76.8, 78.5, 81.0, 83.9, 84.2, 127.0, 127.3, 128.6, 128.8, 129.1, 130.1, 131.7, 133.1, 133.5, 134.2, 138.2, 140.4, 158.0, 167.0, 168.8, 170.5, 172.6, 202.0. Anal. calcd for  $C_{53}H_{60}N_2O_{15}$ : C, 65.96; H, 6.26; N, 2.90. Found: C, 65.77; H, 6.44; N, 2.71.

**FITC-conjugated paclitaxel 9.** 7-Aminocaproylpaclitaxel **7** (25 mg, 0.025 mmol, 1 eq) was dissolved in a mixture of dry pyridine:DMF (1:2, 2 mL). To this solution was added FITC (15 mg, 0.037 mmol, 1.5 equiv) and the contents were stirred at room temperature under nitrogen and in darkness for 2 days. The solution was evaporated to dryness under vacuum at 20 °C and the residual material was washed successively with acetone ( $3 \times 5$  mL) and diethylether ( $3 \times 5$  mL). The crude mixture was purified by preparative TLC on silica gel (EtOAc/ $CH_2Cl_2$ , 1:5;  $R_f=0.45$ ) to give the product **8** as a bright yellow solid (18 mg, 53%).  $^1H$  NMR (400 MHz,  $CD_3OD$ )  $\delta$  1.02 (s, 3H,  $H_{16}$ ), 1.05 (s, 3H,  $H_{17}$ ), 1.27–1.34 (m, 2H,  $CH_2$ ), 1.49–1.54 (m, 4H,  $CH_2$ ), 1.68 (s, 3H,  $H_{19}$ ), 1.69–1.71 (m, 1H,  $H_{6b}$ ), 1.78 (s, 3H,  $H_{18}$ ), 2.03 (s, 3H,  $C_{10}-CH_3CO$ ), 2.01–2.18 (m, 2H,  $CH_2$ ), 2.24–2.39 (m, 2H,  $H_{14}$ ), 2.26 (s, 3H,  $C_4-CH_3CO$ ), 2.41–2.59 (m, 1H,  $H_{6a}$ ), 3.22–3.28 (m, 2H,  $NCH_2$ ), 3.91 (d,  $J=6.0$ , 1H,  $H_3$ ), 4.16 (d,  $J=7.9$ , 1H,  $H_{20}$ ), 4.28 (d,  $J=7.9$ , 1H,  $H_{20}$ ), 4.74 (m, 1H,  $H_2$ ), 4.87 (d,  $J=8.0$ , 1H,  $H_5$ ), 5.45 (dd,

$J=9.8$ , 3.2, 1H,  $H_7$ ), 5.58 (d,  $J=7.6$ , 1H,  $H_2$ ), 5.66 (m, 1H,  $H_3$ ), 6.16 (t,  $J=8.6$ , 1H,  $H_{13}$ ), 6.23 (s, 1H,  $H_{10}$ ), 6.44 (d,  $J=8.0$ , 2H, ArH), 6.52–6.71 (m, 4H, ArH and NH), 7.15 (d,  $J=8.0$ , 1H, NH), 7.23–7.38 (m, 14H, ArH and NH), 7.64 (d,  $J=8.0$ , 2H, ArH), 7.91–8.03 (m, 2H, ArH), 8.18 (d,  $J=8.0$ , 2H, ArH);  $^{13}C$  NMR (100 MHz,  $CD_3OD$ )  $\delta$  11.0, 14.3, 20.5, 20.7, 22.0, 24.0, 26.2, 30.2, 33.0, 33.2, 33.6, 35.4, 43.1, 43.2, 43.5, 47.1, 50.5, 50.8, 54.9, 56.0, 56.6, 71.9, 72.2, 73.3, 74.6, 75.6, 76.3, 78.8, 81.0, 83.5, 84.4, 101.8, 127.1, 127.3, 128.3, 128.6, 128.7, 129.2, 130.8, 131.8, 133.1, 133.5, 134.0, 138.2, 140.2, 142.0, 167.0, 168.5, 170.1, 172.8, 191.9, 202.2. Anal. calcd for  $C_{74}H_{73}N_3SO_{20}$ : C, 65.52; H, 5.42; N, 3.09. Found: C, 65.39; H, 5.69; N, 2.83.

**Lissamine rhodamine B conjugated paclitaxel 11.** To a solution of **7** (16 mg, 0.016 mmol, 1 equiv) in dioxane and saturated aqueous  $NaHCO_3$  (1:1, 2 mL) at room temperature under inert atmosphere was added Lissamine rhodamine B sulfonyl chloride **10** (12 mg, 0.020 mmol, 1.25 equiv) and the reaction mixture was stirred for 36 h. This was then diluted with aqueous NaCl solution (5 mL) and extracted with EtOAc ( $10 \times 10$  mL). The combined organic extract was concentrated under reduced pressure and the residue was purified by TLC on silica gel (1% AcOH and 15% MeOH in  $CH_2Cl_2$ ). The major band ( $R_f=0.6$ ) was scrapped, eluted with EtOAc, and concentrated to give **11** as a purple layer (13 mg, 58%).  $^1H$  NMR (400 MHz,  $CD_3OD$ )  $\delta$  1.05 (s, 3H,  $H_{16}$ ), 1.07 (s, 3H,  $H_{17}$ ), 1.08–1.31 (m, 12H,  $NCH_2CH_3$ ), 1.31–1.48 (m, 2H,  $CH_2$ ), 1.53–1.69 (m, 4H,  $CH_2$ ), 1.81 (s, 3H,  $H_{19}$ ), 1.82–1.84 (m, 1H,  $H_{6b}$ ), 1.86 (s, 3H,  $H_{18}$ ), 2.12 (s, 3H,  $C_{10}-CH_3CO$ ), 2.14–2.31 (m, 2H,  $CH_2$ ), 2.33–2.42 (m, 2H,  $H_{14}$ ), 2.44 (s, 3H,  $C_4-CH_3CO$ ), 2.49–2.65 (m, 1H,  $H_{6a}$ ), 3.31–3.39 (m, 2H,  $NCH_2$ ), 3.81 (t, 8H,  $J=6$ ,  $NCH_2$ ), 3.94 (d,  $J=7.5$ , 1H,  $H_3$ ), 4.19 (d,  $J=7.0$ , 2H,  $H_{20}$ ), 4.79 (d,  $J=3.0$ , 1H,  $H_2$ ), 4.91 (d,  $J=8.0$ , 1H,  $H_5$ ), 5.51–5.73 (m, 3H,  $H_2$ ,  $H_3$ , and  $H_7$ ), 6.22 (t,  $J=9.5$ , 1H,  $H_{13}$ ), 6.28 (s, 1H,  $H_{10}$ ), 7.01–7.04 (m, 2H, ArH), 7.15 (d,  $J=7.6$ , 1H, NH), 7.21–7.38 (m, 5H, ArH and NH), 7.40–7.68 (m, 12H, ArH), 7.69–7.81 (m, 1H, ArH), 8.06 (d,  $J=8.0$ , 1H, ArH), 8.19 (brt, 1H, ArH), 8.68 (brs, 1H, ArH);  $^{13}C$  NMR (100 MHz,  $CD_3OD$ )  $\delta$  11.7, 13.1, 14.7, 20.6, 20.9, 22.3, 23.5, 24.0, 24.4, 25.0, 26.2, 27.1, 30.7, 31.0, 33.1, 34.5, 34.8, 35.6, 36.8, 41.1, 43.0, 43.2, 43.5, 47.0, 50.6, 50.8, 55.0, 56.4, 56.9, 58.1, 72.3, 75.1, 76.0, 76.9, 77.6, 79.1, 82.2, 83.5, 85.4, 97.1, 115.2, 115.3, 115.9, 116.1, 127.3, 128.6, 129.3, 129.9, 130.5, 131.4, 131.8, 133.1, 134.1, 134.2, 134.7, 134.9, 140.2, 142.0, 146.8, 156.9, 157.0, 159.5, 159.9, 167.5, 170.6, 170.9, 171.0, 172.9, 174.7, 176.8, 202.5. Anal. calcd for  $C_{80}H_{91}N_4S_2O_{21}$ : C, 63.68; H, 6.07; N, 3.71. Found: C, 63.92; H, 6.22; N, 3.44.

**Cell culture and fluorescent staining.** The human non-small cell lung cancer cells H460 were obtained from

American Type Culture Collection (ATCC; MD). These cells were grown in RPMI-1640 supplemented with 10% FBS and subcultured 2–3 times/week. The cells were seeded on a cover glass in a density of  $1 \times 10^5$  ml and allowed to grow overnight for attachment. The culture medium was removed and cells on the cover glass were washed three times with PBS. Then, the cells were fixed with ethanol at  $-20^\circ\text{C}$  for 30 min. After fixation, the ethanol was removed and cells were washed three times with PBS. Now  $0.25 \mu\text{M}$  of **9** or **11** was added to the sample and stained for 1 h at  $4^\circ\text{C}$  in darkness. The coverslips were washed extensively with PBS and then mounted in an anti-bleaching mountant (5% propylgallate dissolved in 15% PBS/85% glycerol). The samples were examined under a Zeiss Axiophot microscope equipped with epifluorescence optics and all images were recorded under a Plan-neoflar  $100\times$  (N.A. 1.3) objective.

**Drug accumulation assays.** H460 cells were grown to 70–80% confluence and seeded in 35 mm dishes (Falcon, CA). The cell monolayers were washed with PBS and then incubated with serum free RPMI-1640 medium and **4** (specific activity, 48 mCi/mmol) at  $37^\circ\text{C}$ . At the end of the treatment, the cell monolayers were washed three times with an ice-cold PBS and the cells were lysed with 20 mM Tris-HCl, pH 7.7, containing 0.2% SDS. Radioactivity in the cell lysates was determined by  $\beta$ -scintillation counting.

**Flow cytometric analysis of fluorescent paclitaxel accumulation.** H460 cells were seeded on a 35 mm dish at  $5 \times 10^5$  ml and incubated overnight to attach. The old medium was removed and replaced by fresh medium. The fluorescent-paclitaxel (**9** or **11**) was added to the culture and incubated at  $37^\circ\text{C}$ . At the end of treatment, the cells were washed three times with PBS and followed by trypsinization. The cell suspension samples were kept on ice until they were analyzed. The fluorescence intensity of each sample was quantitated by flow cytometry (FACStar plus, Becton Dickinson, San Jose, CA). The wavelength for excitation was set at 488 nm. The optical filter for emission signal of FITC and rhodamine is 519 nm and 576 nm, respectively. Cell populations of interest were gated according to the forward/side scatter dot plot. The mean channel number of fluorescence intensities of 5,000 cells in each sample tube was determined.

#### Acknowledgements

This work was supported in parts by research grants from the ROC National Science Council (NSC87-2311-B007-028 and NSC87-2311-B007-001-B12) to Y.-K.L. The authors wish to thank Drs. C. Yu and J. Hammond for their valuable comments on this manuscript.

#### References

- Georg, G. I.; Chen, T. T.; Ojima, I.; Vyas, D. M.; Eds.; *Taxane Anticancer Agents: Basic Science and Current Status*; ACS Symposium Series 583; Washington, DC American Chemical Society, 1995; 1–343.
- Horwitz, S. B. *Trends Pharmacol. Sci.* **1992**, *13*, 134–136.
- Ding, A. H.; Porteu, F.; Sanchez, E.; Nathan, C. F. *Science* **1990**, *248*, 370–372.
- Bogdan, C.; Ding, A. H. *J. Leuk. Biol.* **1992**, *52*, 119.
- Manthey, C. L.; Brandes, M. E.; Perera, P.-Y.; Vogel, S. N. *J. Immunol.* **1992**, *149*, 2459–2465.
- Manthey, C. L.; Perera, P.-Y.; Salkowski, C. A.; Vogel, S. N. *J. Immunol.* **1994**, *152*, 825–831.
- Henricson, B. E.; Carboni, J. M.; Burkhardt, A. L.; Vogel, S. N. *Mol. Med.* **1995**, *1*, 428–435.
- Lieu, C.-H.; Chang, Y.-N.; Lai, Y.-K. *Biochem. Pharmacol.* **1997**, *53*, 1583–1596.
- Chu, J.-J.; Chen, K.-D.; Lin, Y.-L.; Fei, C.-Y.; Chiang, A.-S.; Chiang, C.-D.; Lai, Y.-K. *J. Cell. Biochem.* **1998**, *68*, 472–483.
- Parness, J. J.; Horwitz, S. B. *J. Cell Biol.* **1981**, *91*, 479–487.
- Chenu, J.; Takoudju, M.; Wright, M.; Senilh, V.; Guenard, D. *J. Labelled Compd. Radiopharm.* **1987**, *24*, 1245–1255.
- Rao, S.; Horwitz, S. B.; Ringel, F. *J. Natl. Cancer Inst.* **1992**, *84*, 785–788.
- Taylor, G. F.; Thornton, S. S.; Tallent, C. R.; Kepler, J. A. *J. Labelled Compd. Radiopharm.* **1993**, *33*, 501–515.
- Rimoldi, J. M.; Kingston, D. G.; Chaudhary, A. G.; Samaranayake, G.; Grover, S.; Hamel, E. *J. Nat. Prod.* **1993**, *56*, 1313.
- Rao, S.; Orr, G. A.; Ghaudary, A. G.; Kingston, D. G. I.; Horwitz, S. B. *J. Biol. Chem.* **1995**, *270*, 20235–20238.
- Zamir, L. O.; Nedeia, M. E.; Garneau, F. X. *Tet. Lett.* **1992**, *33*, 5235–5236.
- Strobel, G. A.; Stierle, A.; van Kuijk, F. J. G. M. *Plant Science* **1992**, *84*, 65–74.
- Walker, D. G.; Swigor, J. E.; Kant, J.; Schroeder, D. R. *J. Labelled Compd. Radiopharm.* **1994**, *34*, 973–980.
- Walker, D. G.; Standridge, R. T.; Swigor, J. E. *J. Labelled Compds. Radiopharm.* **1995**, *36*, 479–492.
- de Suzzoni, S.; Boullais, C.; Vandais, A.; Noel, J. P. *J. Labelled Compds. Radiopharm.* **1995**, *36*, 739–743.
- Parness, J.; Kingston, D. G. I.; Powell, R. G.; Harrack-singh, C.; Horwitz, S. B. *Biochem. Biophys. Res. Comm.* **1982**, *105*, 1082–1089.
- Mellado, W.; Magri, N. F.; Kingston, D. G. I.; Garcia-Arenas, R.; Orr, G. A.; Horwitz, S. B. *Biochem. Biophys. Res. Comm.* **1984**, *124*, 329–336.
- Takoudju, M.; Wright, M.; Chenu, J.; Gueritte-Voegelein, F.; Guenard, D. *FEBS Lett.* **1988**, *234*, 177–180.
- Ringel, I.; Horwitz, S. B. *J. Pharmacol. Exp. Ther.* **1987**, *242*, 692–698.
- Kingston, D. G. I. *Pharmacol. Ther.* **1991**, *52*, 1–34.

26. Sengupta, S.; Boge, T. C.; George, G. I.; Himes, R. H. *Biochemistry* **1995**, *34*, 11889–11894.
27. Souto, A. A.; Acuna, A. U.; Andreu, J. M.; Barasoain, I.; Abal, M.; Amat-Guerri, F. *Angew. Chem. Int. Ed. Engl.* **1995**, *34*, 2710–2712.
28. Dubois, J.; Le Goff, M.-T.; Gueritte-Voegelein, F.; Guenard, D.; Tollon, Y.; Wright, M. *Bioorg. Med. Chem.* **1995**, *3*, 1357–1368.
29. Guy, R. K.; Scott, Z. A.; Sloboda, R. D.; Nicolaou, K. C. *Chem. Biol.* **1996**, *3*, 1021–1031.
30. Han, Y.; Chaudhary, A. G.; Chordia, M. D.; Sackett, D. L.; Perez-Ramirez, B. Kingston, D. G. I.; Bane, S. *Biochemistry* **1996**, *35*, 14173–14183.
31. Sengupta, S.; Boge, T. C.; Liu, Y.; Hepperle, M.; Georg, G. I.; Himes, R. H. *Biochemistry* **1997**, *36*, 5179–5184.
32. Potier Gueritte-Voegelein, F.; Guenard, D.; Lavelle, F.; Le Goff, M.-T.; Maangatal, L.; P. *J. Med. Chem.* **1991**, *34*, 992–998.
33. Grover, S.; Rimoldi, J. M.; Molinero, A. A.; Chaudhary, A. G.; Kingston, D. G. I.; Hamel, E. *Biochemistry* **1995**, *34*, 3927–3934.
34. Deutsch, J. A.; Glinski, J. A.; Hernandez, M.; Haugwitz, R. D.; Narayana, V. L.; Suffiness, M.; Zalkow, L. H. *J. Med. Chem.* **1989**, *32*, 788–792.
35. Mathew, A. E.; Mejillano, M. R.; Nath, J. P.; Himes, R. H.; Stella, V. J. *J. Med. Chem.* **1992**, *35*, 145–151.
36. Nicolaou, K. C.; Dai, W. M.; Guy, R. K. *Angew. Chem. Int. Ed. Engl.* **1994**, *106*, 15–44.
37. Ponnusamy, E.; Fotadar, U.; Spisni, A.; Fiat, D. *Synthesis* **1986**, 48–49.
38. Mosmann, T. *J. Immunol. Methods* **1983**, *65*, 55–63.